

Enhanced Wound Recovery with Sericin and Morinda citrifolia Leaf Extract Nanogel

Amith Bounsle Nelamangala Ganesha Rao¹, Deveswaran Rajamanickam¹, Basavaraj Basappa Veerabhadraiah¹, Bharath Srinivasan¹, Damodar Nayak Ammunje², Anbu Jayaraman²

¹Department of Pharmaceutics, Faculty of Pharmacy, M.S.Ramaiah University of Applied Sciences, Bengaluru, Karnataka-56054, India

²Department of Pharmacology, Faculty of Pharmacy, M.S.Ramaiah University of Applied Sciences, Bengaluru-560054, Karnataka, India
Email: amithng10@gmail.com

Background: Healing of wounds is a complex process influenced by numerous factors. Different medications can affect clot formation, decrease inflammation, and hinder cell growth during the healing process.

Purpose: Development and assessment of a nanogel incorporating a polyherbal extract of Morinda citrifolia leaf and Sericin protein from silk cocoons to accelerate wound healing.

Methodology: Morinda citrifolia leaf extract was obtained through Soxhlet extraction with ethanol, whereas sericin was extracted from silk cocoons by autoclaving. Extract and polymer compatibility studies were carried out by ATR-IR, and modified solvent-diffusion technique was used to prepare nanogels. The physicochemical properties, drug permeation, scratch assay, cytotoxicity in HDF cells, and in vivo studies were carried out for the developed nanogels.

Results: The Morinda citrifolia leaf extract exhibited a yield of 50-60%, whereas the sericin extract yielded 40-50%. The ATR-IR study showed the absence of interactions between the extract and excipients. Optimal size of the extracted nanogel was 40 nm, with PDI ranging from 0.1-0.6 and exhibiting acceptable physical characteristics. The nanogel demonstrated good cytotoxicity and scratch assay showed enhanced wound healing activity than the standard and control groups. Furthermore, the percentage of wound contraction after excision and incision with hydroxyproline level was greater in rats treated with the nanogel than in those in the negative control group.

Conclusion: The study provides an insight into use of Morinda citrifolia leaf extract and sericin in formation of a nanogel and the developed nanogel was found to be stable, safe, and exhibited promising wound healing activity.

Keywords: cytotoxicity, morinda citrifolia leaf, nanogel, sericin, starch assay, wound healing activity.

1. Introduction

Skin plays a significant role in determining a person's overall attractiveness, as it covers the entire body and is typically the first feature that people notice. Wounds can disrupt the continuity of living tissues, including the skin, by triggering injury to the cellular, anatomical, and functional levels [1-3]. Open wounds are created by tears, cuts, or punctures, whereas closed wounds are caused by blunt force trauma. Burn injuries can result from various sources such as fire, heat, radiation, toxic substances, electricity, and sunlight exposure [4-5]. The process of wound healing entails the restoration of damaged tissue to its original state by mending cellular components and tissue layers. This complex process commences during the fibroblastic stage, which is characterized by cell-to-cell and cell-to-matrix signaling and wound shrinkage [6-7]. The process is divided into different phases such as hemostasis, inflammation, proliferation and remodeling. The second phase is marked through vasoconstriction and platelet aggregation, leading to blood clotting, hemostasis, and phagocytosis, ultimately resulting in inflammation. During the proliferative phase, epithelialization, angiogenesis, and collagen deposition occur, during which fibroblasts produce essential substances for wound repair, such as glycosaminoglycans and collagen. The maturation phase is characterized by wound contraction, leading to less apparent scarring. The proliferative phase, close to its end, results in the development of granulation tissue, comprised of fibroblasts, collagen, and fresh blood vessels [8-9]. The content of hydroxyproline in granulation tissue is directly linked to collagen turnover, ultimately impacting wound strength [10-12].

Old traditional medicine has a significant part in preserving health worldwide. Noni is common name of *Morinda citrifolia*, which has been utilized in ancient medicinal technique to cure various health issues due to its medicinal properties [13–14]. This plant has been found to contain over 160 nutraceutical compounds and has yielded approximately 200 phytochemicals that have been extracted from its various [15]. Various sections of *Morinda citrifolia* used as herbal remedies to treat a wide range of medical conditions [16–17]. The availability of dependable data to determine the safety of noni and its potential skin-related side effects is currently insufficient. *Bombyx mori*, a silkworm from the order Lepidoptera and family Bombycidae, generates a protein called sericin [18]. Sericin is a natural hydrophilic protein found in the silkworms. Sericin's high hydroxyl amino acid concentration make it a promising ingredient for skin moisturizers [19–20]. Nanotechnology presents numerous opportunities for drug delivery, including disease prevention, diagnosis, and treatment [21–22]. This innovative method addresses various challenges by improving drug absorption, prolonging drug release, regulating drug release, and reducing drug toxicity. By applying nanotechnology to medicine, researchers have developed nanoparticles that serve as carriers for medications or genetic materials, which are then released in a controlled or sustained manner to specific target areas [23–24]. Various nanotechnological techniques are currently available for drug delivery, such as nanoemulsions, nanosuspensions, nanotubes, and nanogels [25–26]. Nanogels are a type of hydrogel dispersion created by cross-linking polymers at the nanoscale, resulting in particles between 20 and 200 nm in size [27–28].

In this study, *Morinda citrifolia* leaf extract and sericin from *Bombyx* silk cocoons were formulated into nanogels using Carbopol and HPMC as polymers and subsequently assessed for its wound healing efficacy by *in vivo* studies.

2. Material and Methods

Fresh *Morinda citrifolia* leaves were collected from New Life Herbal Products, Nanjangud, and it was authenticated by a botanist from Foundation for Revitalisation of Local Health Traditions, Bengaluru. Fresh *Bombyx mori* silk cocoons were obtained from the Government Cocoons Market, Ramanagara, Karnataka and authenticated by the Sericulture Department, Bangalore. Ethanol was sourced from Rankem, India, while PEG was purchased from S. D. Fine Chem Ltd. Carbopol 940 was obtained from Loba Chemie Pvt. Ltd. and HPMC K15 was procured from Yarrow Chem, Mumbai. Triethanolamine oleate was procured from merck Life Science Pvt. Ltd. All other chemicals utilized were of analytical grade, while demineralized water was employed.

Morinda citrifolia leaf extraction

The leaves of *Morinda citrifolia* were thoroughly cleaned, shade dried, and then grounded to granular size powder using a mixer. The powder was passed through BSS#60 and then stored in an airtight container. 100g of the powdered leaf was packed in the thimble of and subjected to soxhlet extraction for 72 h using ethanol as solvent. The resulting extract was filtered and evaporated to obtain a solid residue, which was stored in a vial for further use. The extracted compounds were analyzed using standard pharmaceutical procedures.

GCMS studies

The analysis of the ethanolic extract of *Morinda citrifolia* leaves was performed using a gas chromatography-mass spectrometry (GC-MS) system (Agilent GC-MS - CH-GCMSMS-02) [29]. The instrument's initial temperature was set to 50°C and maintained for 2 min before being increased to 280°C at a rate of 6°C/min and held for an additional 5 min. The injection port temperature was set at 250°C, and the helium flow rate was set at 1 mL/min. The gas chromatograph was connected to a quadrupole mass analyzer with a DB 5 MS column that had dimensions of 30 mL x 0.25 mm ID x 0.25 mm film thickness. The samples were injected in split mode at a volume of 1 µL, and the mass spectral scan range was set from 30 to 700 m/z.

Preparation of sericin extract

10 g of cocoons was suspended with 500 ml of sterile distilled water. The flask was then heated to 120°C for 60 min. The resulting sericin solution was centrifuged for 15 min at 5000 rpm. The supernatant was discarded, and the sericin that settled at the bottom was collected and refrigerated at 4°C for 24 h and subjected to lyophilization to obtain a dry sericin powder [30].

Molecular weight determination of sericin by MALDI-TOF

Molecular weight was determined using a MALDI-TOF MS system, which acquired data from Analyser software (Bruker Daltonics, IISC, and Bangalore) [31].

ATR-FTIR analysis

The powders of *Morinda citrifolia* leaf extract and sericin was subjected to Attenuated Total Internal Reflectance (ATR) attachment for the Bruker Alpha II FTIR spectrometer, which was linked to a computer equipped with Opus 7.8 analysis software. The samples were scanned in the range of 400-4000 cm⁻¹ for analysis.

Nanogel Preparation

Nanogel was prepared by modified solvent diffusion method in four stages. Briefly specific quantity of the extract was dissolved in a blend of ethanol and propylene glycol by stirring to form the organic phase. The aqueous phase comprises of dispersion of polymers, carbopol-940 and HPMC. The dispersion was prepared by mixing for 20 min using a magnetic stirrer. The extract mixture was sonicated for 10 min using an ultrasonic system. The extracts were introduced gradually into the aqueous phase via high-speed homogenization using ultrasonic processor for 30 min at a speed of 6000 rpm. This procedure leads to the dispersion of the emulsion into nanodroplets, resulting in the formation of an oil-in-water emulsion. The final stage involved adding triethanolamine while continuously stirring the homogenized o/w emulsion for an hour at 8000 rpm. [32-35]. The nanogel formulations is depicted in the (Table 1).

Table 1. Composition on the formulation of Nanogel.

Ingredients	F1	F2	F3	F4	F5	F6
Morinda citrifolia extract (gm)	2.5	2.5	2.5	2.5	2.5	2.5
Extracted Sericin (gm)	2	2	2	2	2	2
Carbopol 940(mg)	0.3	0.6	0.9	-	-	-
HPMC (mg)	-	-	-	0.8	1.6	2.4
Ethanol (ml)	10	10	10	10	10	10
Propylene glycol (ml)	4	4	4	4	4	4
Triethanolamine (ml)	qs to pH5.5					
Water	qs to 100gm					

Evaluation of prepared Nanogels

The physical properties of the nanogel, such as yield and pH, were evaluated using a digital pH meter (Labman model-LMPH-10, India) [36-37]. Viscosity was determined using a Brookfield viscometer (Brookfield Engineering Labs, LVDVII) at Spindle IV at 25 °C [38]. The spreadability of the nanogel was assessed using a spreadability apparatus [39]. The swelling behavior was examined in different pH buffers (0.5M buffer solution at pH 1.2 and 7.4) at various time intervals [40]. The nanogel was analyzed for its water absorption percentage, which was determined by immersing it in 200 mL of distilled water at 37°C for 24 hours, as per the equation mentioned in [41]. The spreadability, swelling behavior, and percentage water absorption were determined using specific equations.

$$\text{Spreadability} = m\left(\frac{l}{t}\right)$$

Where

S= Spreadability

m= upper glass slide weight (20g)

l=glass slide length

t= time taken(Seconds)

$$[\text{Swelling} = \frac{w_2}{w_1}]$$

Where

w1= initial weight of Nanogel

w2= Final weight of nanogel

$$\% \text{ water absorption} = \frac{\text{weight before soaking} - \text{weight after soaking}}{\text{weight before soaking}} * 100$$

Estimation of flavonoids and protein content

The extraction of flavonoids from *Morinda citrifolia* leaves and the quantification of sericin protein in silk cocoons were evaluated using a UV-visible spectrophotometer at wavelengths of 415 and 750 nm, respectively. In conducting the assessment, a nanogel formulation was dispersed in a phosphate buffer with a pH of 7.4, passed through a membrane filter, and its absorbance was measured at a designated wavelength using a UV-visible spectrophotometer [42].

In vitro drug permeation studies

Franz diffusion cell was utilized, where receptor compartment containing 15 mL of pH 7.4 phosphate buffer solution. Between donor and receptor compartments, a rat skin was clamped in place with 1g of nanogels applied onto it. The apparatus was subsequently placed on a thermostatically controlled hot plate that was equipped with a magnetic stirrer and maintained at a temperature of $37 \pm 20^\circ\text{C}$. The contents was stirred at 100 rpm for 24 hat various time, 1 mL of each sample was collected and diluted with buffer, and the protein and flavonoid contents were measured at 750 and 415 nm, respectively, using a UV-Visible spectrometer [43].

Polydispersibility and particle size study

The size and polydispersity index of the nanogel were examined using the Dynamic Light Scattering (DLS) method and a Zetasizer. The measurements were taken at a scattering angle (90°) and temperature (25°C) in triplicate. The zeta potential was calculated to evaluate the stability of the prepared nanogel.

Scanning electron microscopy

Nanogel was placed on a 10 mm glass slide and allowed to dry overnight in a vacuum desiccator at room temperature. The slide was attached to a support and coated with gold using a gold-sputter module. The scanning electron microscope (SEM) images were captured using a Zeiss Ultra 55 instrument. The operating voltage of the instrument was set at 15 kV, and multiple magnifications were used to capture the images.

Measurement of nanogel rheology

Rheological measurements were performed using Anton Paar (Rheolab, Anton Paar). 1 g of each sample was subjected to compression between a 1 millimeter gaps. Steady shear experiments were carried out to determine the viscosity and shear stress of the samples at various shear rates ranging from 1 to 100 S^{-1}

Cytotoxicity test

The viability of human dermal fibroblast (HDF) cells exposed to nanogels was evaluated using the MTT assay, which employs 3-(4, 5-dimethylthiazol-2-yl)-2, 5-diphenyltetrazolium bromide as the testing agent. The MTT assay was conducted by seeding 200 μL of cell suspension at a density of 20,000 cells/well in a 96-well plate for 24 h in the absence of the test agent. Afterward, the test agents were added at their respective concentrations, and the plate was incubated for an additional 24 h at 37°C in a 5% CO_2 atmosphere. Subsequently, the incubation period, the spent media was removed, and MTT reagent was added to a final concentration of 0.5 mg/mL. The plate was then wrapped in aluminum foil to prevent exposure to light, and the MTT reagent was incubated for 3 h. After removing the MTT reagent, a solubilization solution was added, and the absorbance was measured at 570 nm using a spectrophotometer or ELISA reader [44].

Wound scratch assay

Cells from the HDF line were initially seeded at a concentration of 3×10^6 cells/mL in 24-well plates and allowed to grow for 24 hours at 37°C and 5% CO_2 . To create a standardized scratch in the confluent monolayer, a sterile p200 pipette tip was used to scrape the surface gently. The purpose of this procedure was to ensure consistent size and distance for all samples. After rinsing the cells with PBS to remove debris, media containing different treatment solutions (methanolic, ethanolic, and aqueous extracts) were added at a concentration of 50 $\mu\text{g/mL}$. The study utilized Cipradin as the positive control, while untreated cells served as the negative control. The purpose of the study was to evaluate wound closure by taking images of migrated cells using a digital camera connected to an inverted microscope at both 0 and 24 hours [45].

In Vivo Studies

The research was carried out in accordance with the moral principles established by the Institutional Animal Care and Use Committee (IAEC) and was authorized before commencement under the identification number XXV/MSRFP/CEU/M-015/221.10.2021. The National Institutes of Health's recommendations for the care and management of experimental animals were followed scrupulously during the entire study.

Dermal Irritation test

Adhering to the OECD 404 guidelines, a dermal irritation test was carried out on rabbits prior to conducting wound healing studies. A 6 cm^2 area on the dorsal region of each rabbit was shaved and utilized as the application site for the topical test formulation. The untreated area of each rabbit acted as the control. After a period of 4 h, the test substance was removed, and 14 days animals were observed to identify any signs of edema, erythema, redness, or inflammation [46].

Wound healing activity

A study on the effectiveness of nanogels in wound healing was conducted using wound models (excision and incision) [47]. Wistar rats were divided into six group (total of 36 male wistar rats of 8 weeks old), with each group designated as groups I, II, III, IV, V, and VI. Here I, IV are control groups, Group II, V are treated with marketed gel, whereas Group III and VI are treated with Optimized nanogel formulation (F3). Before wound induction, using mixture of

ketamine and xylazine (80 mg/kg and 20 mg/kg, i.p., respectively, based on body weight) rats were anesthetized. The skin of the rats was shaved a day before the experiment, and 8 mm of the skin was removed from the excision wound groups (I,II,III) at a depth of 2 mm from the predetermined shaved area. A full-thickness paravertebral incision of 6 cm length, including the cutaneous muscles of the depilated back of each rat, was made to create an incision wound in the group (IV, V, and VI). The wounds were left uncovered and exposed to an open environment, and normal saline solution was applied to achieve hemostasis. The injured animals were housed separately in different cages to monitor signs of infection [48]. Throughout the treatment phase, the wound dimensions were assessed on days 0th, 3rd, 5th, 7th, 10th, 12th, 14th, 17th, and 21st days for excision wounds and on day's 0th, 3rd, 5th, 7th, 10th, and 13th days for incision wounds. The wound contraction formula provided below was used to calculate wound contraction [49].

$$\% \text{ Wound Contraction} = \frac{\text{wound area (Initial)} - \text{wound area (Specific Days)}}{\text{wound area (Initial)}} * 100$$

The Graph Pad Instat software (Version 3.1, GraphPad Software, Inc.) was utilized for the statistical analysis of the results, which included a two-way ANOVA with a post-test and Tukey-Kramer multiple comparison test. The analysis showed that all ratings were statistically significant ($p < 0.001$) according to the results.

Following research period, Wistar rats from each group were euthanized, and the healed portion of the wounds was removed, leaving a 5 mm margin around the edges. The obtained skin tissues were subjected to histopathological and biochemical examination.

Histopathological Analysis

Tissue samples were collected, preserved in formalin, and stored at -70°C for future analysis. The skin samples underwent various histological processing steps, such as embedding, sectioning, staining, and visualization under a microscope connected to a camera (Labomed Lx300) [50].

Biochemical assay

Biochemical assays, such as measuring the levels of hydroxyproline, can be used to assess wound healing. To accomplish this, 0.1 mL of hydrolysate sample is transferred to a sterile test tube and diluted with 0.5 mL of distilled water to a total volume of 0.5 mL. Next, a standard solution of hydroxyproline is diluted to 100 mL, and 0.5 mL (8 mg) is added to the test tube. Subsequently, 1 mL of 2.5 N NaOH, 0.01 M CuSO₄, and 6% H₂O₂ is added, followed by heating the test tube in a water bath at 80°C for 16 min and then allowing it to cool for 5 min. Next, the test tube is treated with 2 mL of 5% para-dimethylamino-benzaldehyde in n-propanol and 4 mL of 3 N H₂SO₄ in a similar manner with repeated heating and cooling steps. Finally, the resulting color is compared to a standard color chart at 540 nm using a UV-vis spectrophotometer to determine the amount of hydroxyproline present [51].

Stability studies

The nanogel was stored for six months with a temperature of at 40±2°C and 75±5% RH, according to ICH guidelines, to assess its stability. The optimized nanogel was evaluated by collecting samples at 0, 2, 4, and 6 months for visual inspection, pH, spreadability, and drug

content analysis. This was done in accordance with established protocols [52].

Statistical Analysis

In this research, the data was expressed as the mean \pm standard deviation (SD). Statistical analysis of the obtained data was conducting using Microsoft Excel.

3. Results and Discussion

The percentage yield of morinda citrifolia leaf extract was 18.53% with reddish brown colour and sericin was lightly yellowish in colour with 7.9%. Preliminary phytochemical screening of morinda citrifolia leaf extract revealed the presence of alkaloids, glycosides, flavonoids, phenolic compounds, tannins and fixed oils, whereas mucilage, proteins and aminoacids were absent in morinda citrifolia leaf extract.

GC-MS analysis

The evaluation of GC-MS data was carried out using the NIST database from the National Institute of Standards and Technology. The spectrum of the unknown components was contrasted with that of the known components in the NIST library, and the identification of 35 compounds is illustrated in (Figure 1a).

MALDI-TOF MS results

The molecular weight of sericin was 5798.093 m/z (Figure 1b). This indicates, that it is a low-molecular-weight sericin utilized for wound healing, as stated by Seo et al.,2023 [54].

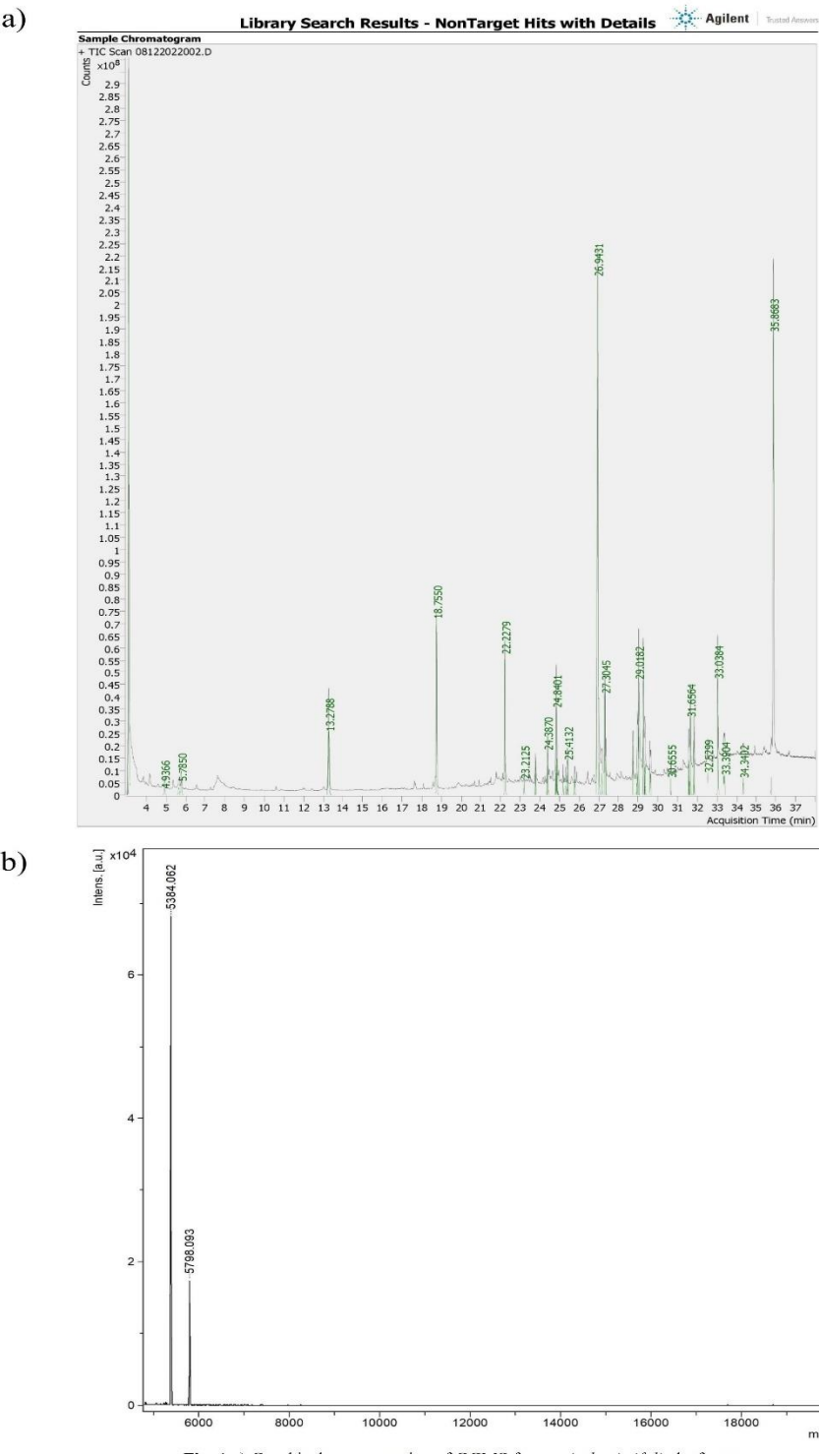


Figure 1 a) Graphical representation of GCMS for morinda citrifolia leaf extract

Nanotechnology Perceptions Vol. 20 No. S8 (2024)

b) Graphical representation of MALDI-TOF test for sericin

ATR-FTIR studies

The ATR-FTIR spectra for the *Morinda citrifolia* leaf and sericin extracts, carbopol 940, HPMC, and the physical mixture of these extracts and excipients are presented in (Figure S1), and the interpretations are provided in (Table S1). Notably, no significant differences were observed between the ATR-IR spectra of the physical mixture and those of the pure extracts and excipients, suggesting the absence of any interactions between them. After conducting the preliminary studies, the nanogel was prepared and subjected to physical evaluation.

Evaluation of prepared Nanogel

The evaluation of the prepared nanogel is shown in (Table 2), which includes parameters, such as percentage yield, pH, spreadability, and percentage water absorption. The pH of the nanogel was within an acceptable range of 6.0 ± 0.012 , making it suitable for topical application. According to the report by Al-Hamadani et al., (2021) [52], the viscosity of the nanogel formulation is influenced by the concentration of the polymer or gelling agent. Rheogram results showed that the nanogel exhibited shear thinning, with a decrease in viscosity as the RPM increased as reported in (Figure 2a) and this property is preferred in topical preparations. The spreadability of the nanogel was found to be within the range of 23.21 ± 2.47 g.cm/sec, and it displayed an inverse relationship with viscosity. Swelling studies with the 7.4 buffer showing a higher output owing to the ionized forms of hydroxyl and carboxylic groups at alkaline pH, resulting in greater electrostatic repulsion and more space within the network, as depicted in (Figure 2b). The high water absorption of the nanogel was attributed to its large pore capacity, which increased with increasing polymer concentration. The nanogels absorbed more water as the polymer concentration increased, resulting in even greater enlargement.

Extract content

The concentration of flavonoids and sericin in the pure extract was measured to be 76.08 ± 1.20 mg/g and 138.38 ± 1.3 mg/g, respectively. The levels of these compounds in the formulated nanogel are provided in (Table 2), which indicates that the flavonoid content ranged from 72.37 ± 1.22 to 85.40 ± 1.06 mg/g for *morinda citrifolia*, while the sericin content ranged from 72.50 ± 1.2 mg/g to 84.13 ± 0.7 .

In vitro drug permeation studies

The purpose of the In vitro release studies was to evaluate the release behavior of flavonoids and sericin from the nanogels. The release graphs are illustrated in (Figure 2c), which indicated that both flavonoids and sericin released 40% of their content after 8 h. This suggests an initial burst release, followed by 92% and 84% release of flavonoids and sericin, respectively, after 24h due to the sustained release properties of the nanogel. This was attributed to the uniform dispersibility of the crude extract in the nanogel and the polymer concentration, as reported by Rao Avanapur et al., [43].

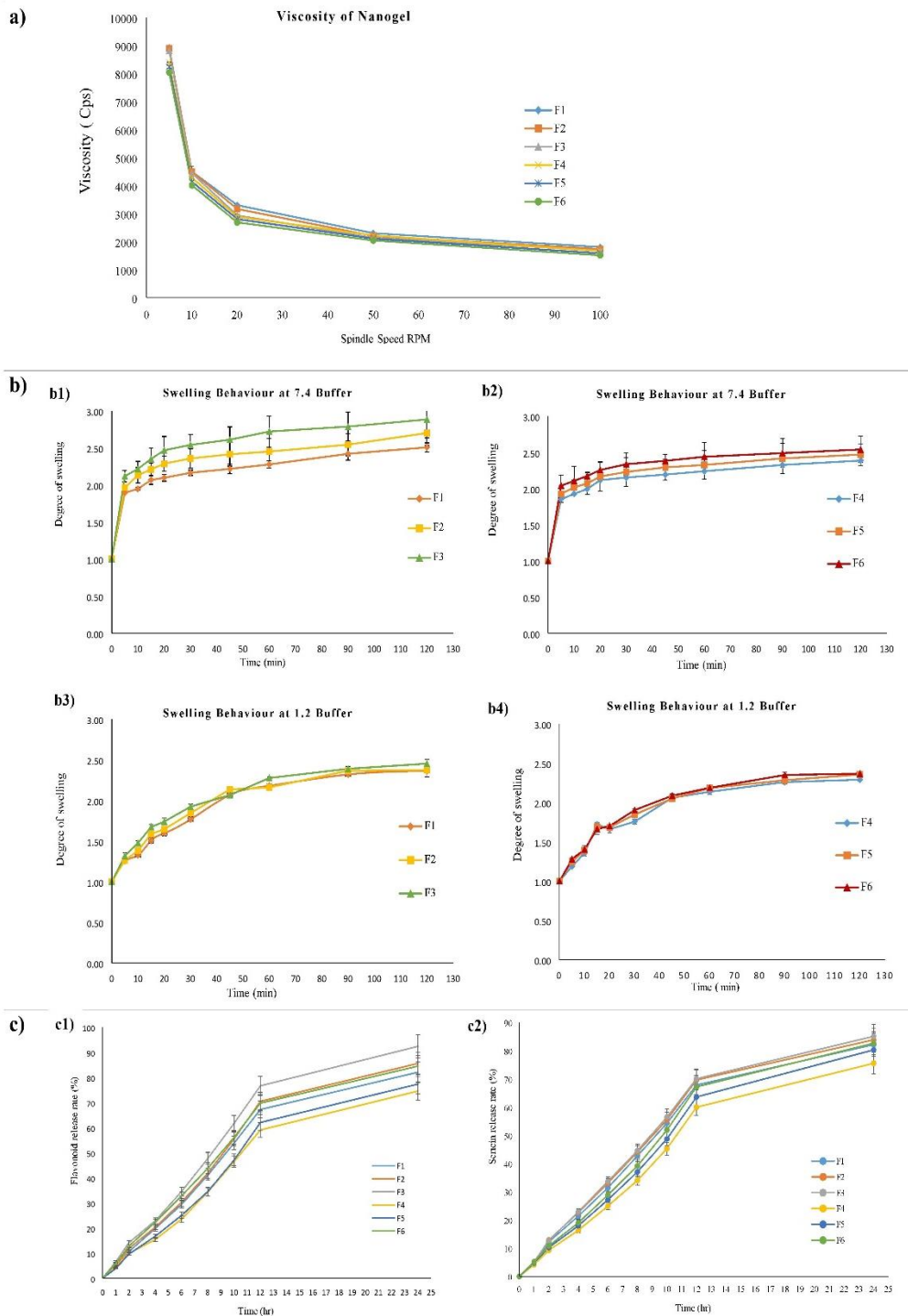


Figure 2 a) Graphical representation between Viscosity and RPM.

b) The graphical representation of swelling vs. time, b1) and b2) represents swelling behavior of formulation F1 to F6 in 7.4 buffer. b3) and b4) represents swelling behavior of formulation F1 to F6 in 1.2 buffer

c) The graphical representation, c1) % Flavonoid release vs. Time c2) % sericin release vs. Time

Table 2. Evaluation parameters of nanogel formulations

Formulation	Yield [%]	pH	Spreadability (gm.cm/sec)	water absorption [%]	Flavonoid content [%]	Sericin content [%]	Polydispersibility	Zeta Potential [mV]	Particle Size (Diameter) nm
F1	98.4	6.05±0.01	26.7± 2.9	12.6 ± 0.2	81.6 ± 0.2	78.5 ± 0.5	0.175	-35.52	405.8
F2	98	6.03±0.01	23.8 ± 2.8	13.4 ± 0.2	81.8 ± 0.9	82.4 ± 0.6	0.303	19.52	673
F3	98.8	6.52±0.01	28.3 ± 2.3	14.6 ± 0.1	85.4 ± 1.1	84.1 ± 0.7	0.283	-40.66	46.83
F4	96	5.93±0.02	22.6 ± 2.1	12.8± 0.1	72.4 ± 1.2	72.5 ± 1.2	0.263	46.87	591.3
F5	98.2	5.42±0.01	21.7 ± 3.1	13.9 ± 0.1	76.5 ± 1.7	78.5 ± 0.5	0.202	-29.83	839.4
F6	97.2	5.14±0.04	20.5 ± 1.5	15.3 ± 0.1	81.3 ± 0.9	80.1 ± 0.9	0.652	-8.05	1164.4

Polydispersibility index and particle size study

Polydispersibility and Particle size were measured, with the results shown in (Table 2). The PDI for all nanogel compositions ranged from 0.1 to 0.6, indicating a relatively broad distribution of particle size. Nanogels were recorded with zeta potential for all compositions, with the lowest zeta potential value of -8.05 and the highest value of 46.87. The particle diameter with the optimised nanogel was 46.83 nm. The image illustrating the polydispersibility and zeta potential is depicted in (Figure S2). Based on the above studies, nanogel Formulation F3 demonstrate to have the most favorable outcomes and was subsequently selected for SEM and In-vivo investigations.

Scanning electron microscopy

The particles in the nanogel were moderately spherical in shape, with a smooth surface, and possessed a particle size within the nanometric range, as evidenced by the SEM image shown in (Figure 3a).

Rheological study

The purpose of gels in applications is to exhibit pseudoplastic behavior, which is characterized by a decrease in the apparent viscosity as the shear rate increases, as shown in (Figure 3b). This property is essential for easy application of the tube to the intended site. In addition, the gel should be sufficiently viscous to remain at the applied location, such as the skin, as reported by Abdul Rahman et al., [56].

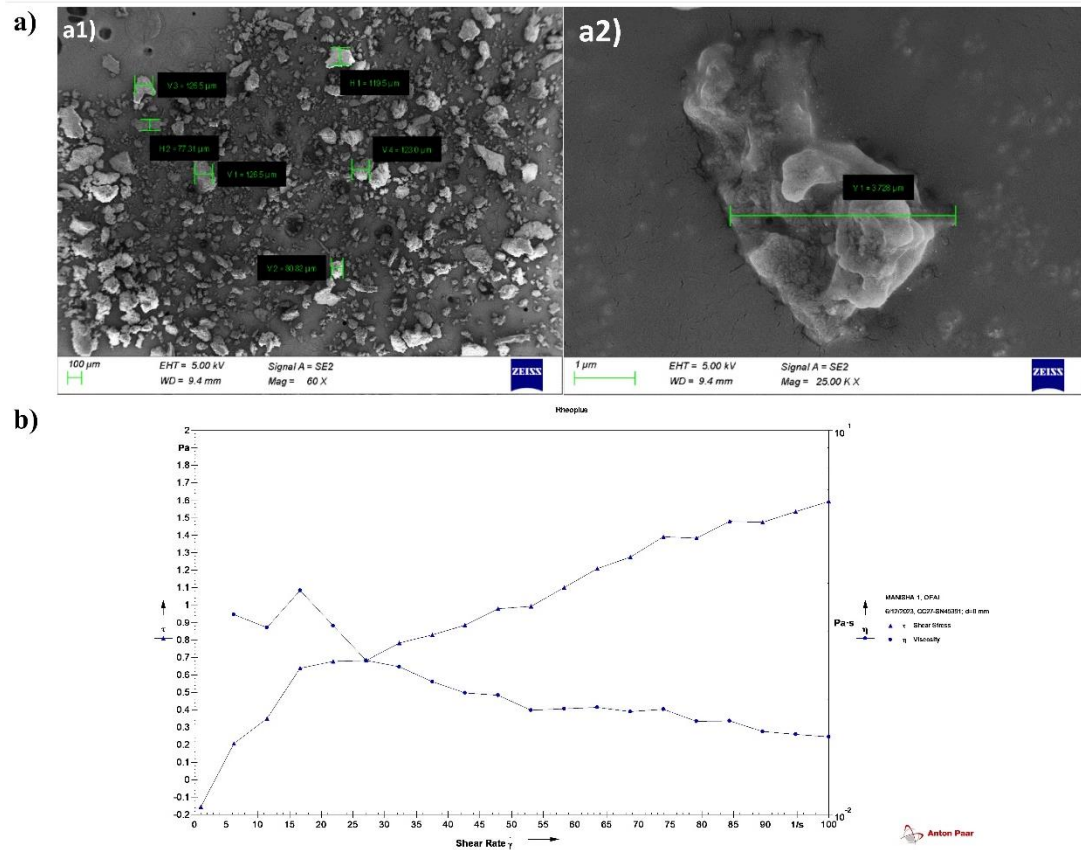


Figure 3 a) SEM Image of optimized nanogel b) Graphical representation on shear rate vs. shear stress and viscosity

Cytotoxicity test

MTT assay shown the % cell viability in HDF cells with varying concentrations of nanogel. The results demonstrate that the control group, as well as the standard drug doxorubicin and prepared nanogel (F3) samples at all concentrations tested, exhibited no cytotoxicity towards the HDF cells. Notably, the cells showed a maximum viability of 135% at the highest nanogel concentration (F3) by increasing the concentration percentage of viability also increased as stated by the report Syarina et al., [45]. The % cell viability HDF cell ith varying concentrations of nanogel are shown in (Figure 4a). Microscopic observations of the formulation-treated images of HDF cells captured at 20x magnification after 24 h of incubation are shown in (Figure S3).

Wound healing scratch assay

The progression of wound closure in scratch-wounded HDF at 0, 24, and 48 h post-injury, with and without treatment was assessed. The images display the effects of the prepared nanogel (F3) treatment on cell migration and wound closure compared to untreated cells and the standard control (Cipladin) as reported by Syarina et al., [45]. These molecules

considerably improved the rate of wound healing in HDFs in a time-dependent manner, achieving a higher wound healing rate than both the control and standard (cipladin), as illustrated in (Figure 4b). The outcomes of the wound healing scratch assay demonstrated that the Nanogel (F3) formulation prepared exhibited an excellent wound healing effect. (The Figure S4) show the progression of wound healing in scratch-injured human dermal fibroblasts (HDF) at 0, 24, and 48 hours after injury, both with and without treatment.

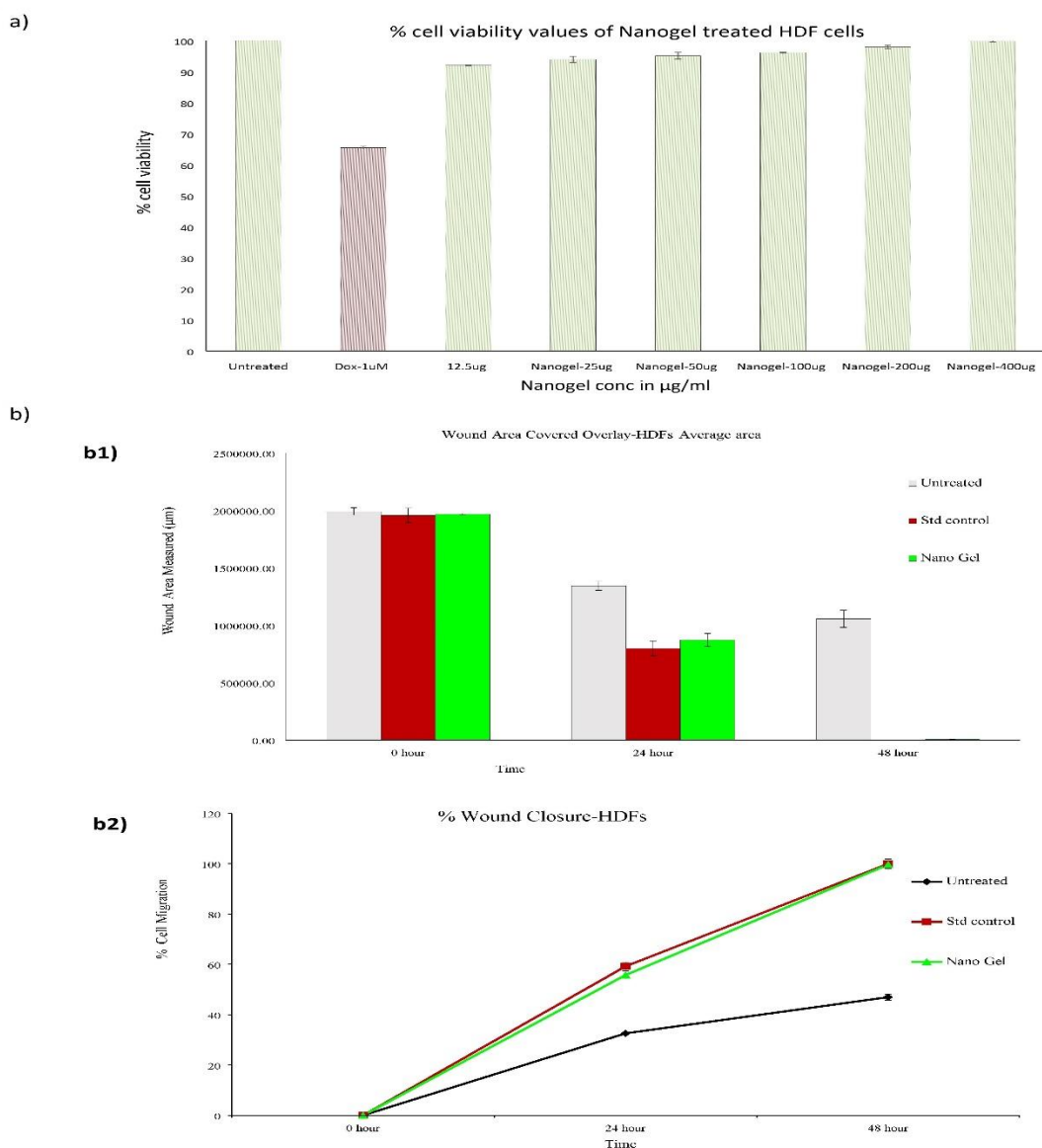


Figure 4. a) Graphical representation of % cell viability of Nanogel with different concentration on HDF cell in comparison with untreated and standard doxorubicin b) Graphical representation of scratch assay in which b1) represents overlaid bar graph of wound area covered with nanogel and b2) represents % wound healing effect of nanogel

Skin irritation study

Skin Irritation study in rabbits demonstrated that the nanogel was safe for topical application, as no irritation were observed after two weeks with zero scores. Additionally, no edema or erythema was observed at the application site, suggesting that the optimized nanogel is a safe and efficient option for skin care.

Wound healing activity by Excisional and Incisional wound model

The current research indicates that the nanogel-based delivery system for the extracts has proven effective in promoting wound healing. Throughout the course of the trial, no adverse events, including granulation tissue bleeding, fluid accumulation, infection, sepsis, or other complications, were observed in any of the rats. All animals survived until the conclusion of the study, and by the third week, all groups had fully recovered. The wound contraction area following excision and incision is illustrated in (Figure 5 a1), while (Figure 5 a2) shows the structural and morphological changes resulting from incision. A simple marketed formulation was used to treat animals in the wound model. The results indicated that there was no statistically significant difference in the wound contraction area between the excision group and the negative control group (untreated group) from days 0 to 5. However, on day 7, there was a small but statistically significant difference ($p=0.0105$) in the wound area. On day 10, the difference became more statistically significant ($p=0.0012$). From day 12 onwards, there was a drastic and statistically significant difference ($****p<0.0001$) in the wound area. In contrast, the nanogel showed a small but statistically significant change in wound area on day 3 ($*p=0.0173$), followed by a drastic and statistically significant reduction in wound contraction area from day 5 ($****p<0.0001$), and wound healing on day 14. In contrast, the marketed gel exhibited wound healing on day 17. The results from the incision model on animals treated with both the marketed formulation and Nanogel showed no statistically significant difference in the wound contraction area compared to the negative control group (untreated group) from days 0 to 3. However, on day 3, the marketed formulation showed a small but statistically significant change in wound area ($p=0.0101$), and on day 5, there was a more statistically significant change ($p=0.0022$). From day 7, there was a drastic and statistically significant change in the wound area ($p<0.0001$). Unlike the marketed product, the nanogel demonstrated a remarkable and statistically significant decrease in the wound contraction area from day 5 onwards ($p<0.0001$). Moreover, the percentage wound contraction was significantly greater for the prepared nanogel compared to the marketed product for both excision and incision studies, as illustrated in (Figure 5b).

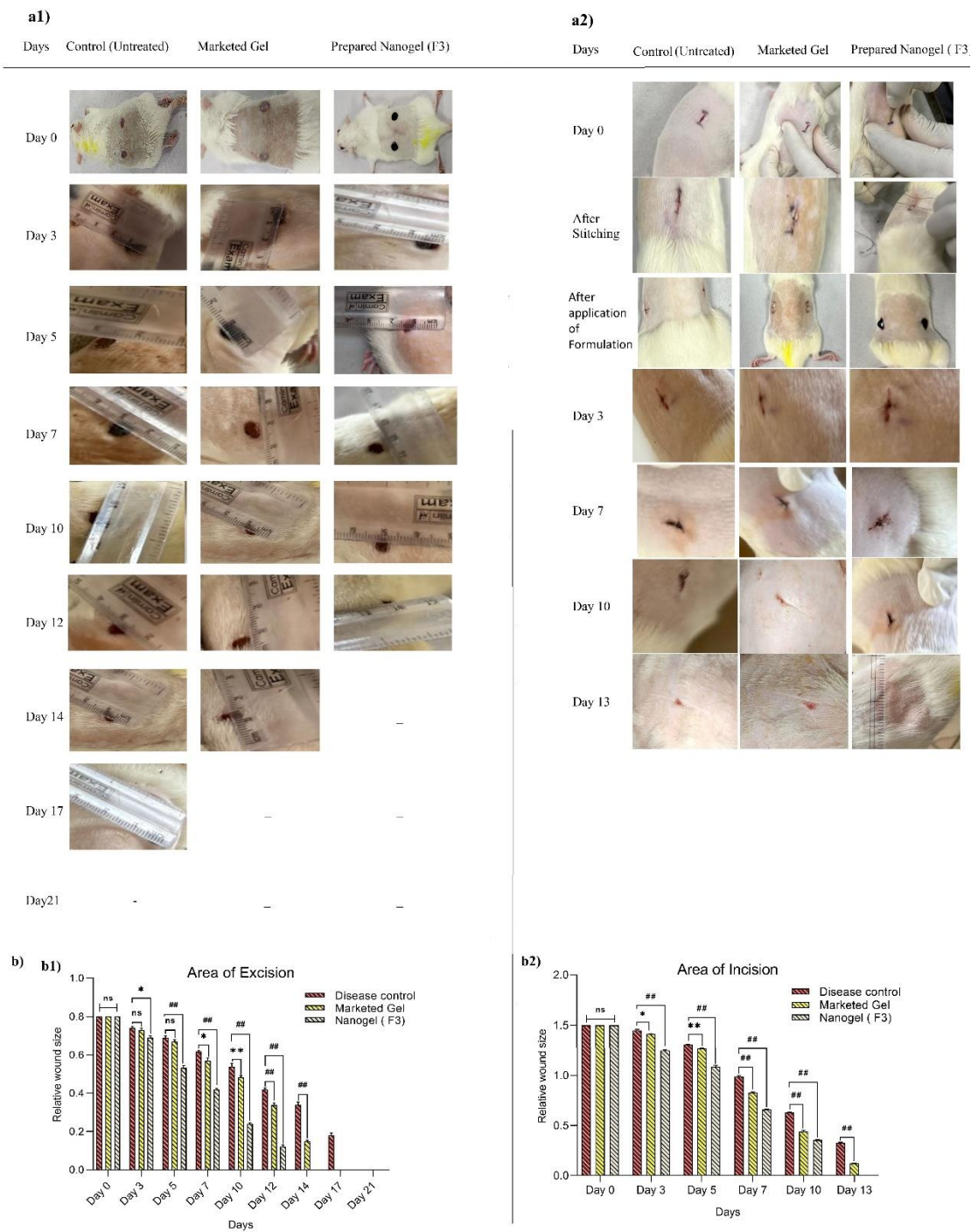


Figure 5. a) Photographs of wound repair at different time interval in a1) excision & a2) incision wound model in rat comparing with marketed against control b) Graphical representation of relative wound contraction in both b1) excision & b2) incision wound

model against different time intervals in comparison with marketed against disease control

Histopathological Analysis

Histopathological examination of tissue samples from the excision and incision wounds was conducted on day's 21st and 13th days, respectively. The histopathological features of the tissue samples from all the animal groups are shown in (Figure 6). In the excision wound model, the section of group I (control) animals showed the presence of inflammatory cells, extracellular matrix in the entire wound area (identified by a few fibroblasts), and thin collagen fibers on the skin. Group II (marketed gel) exhibited hyperkeratinization and congestion, with glandular hyperplasia. Group III (prepared nanogel) demonstrated an extensive healing response, as evidenced by keratinocytes with glandular proliferation and dermal region collagen with ECM proliferation. In the incision wound model, the sections of group IV (control) animals showed epidermal layer hyperkeratinization, inflammation, congestion in the dermis, follicular hyperplasia, and reduced collagen fibers. Group V (marketed gel) exhibited hyperkeratinization with glandular proliferation, granulation, and inflammation. Group VI (prepared nanogel) demonstrated an extensive healing response, as evidenced by keratinocyte glandular proliferation and dermal region angiogenesis with ECM proliferation. Based on the histopathological analysis of both excision and incision studies, it can be concluded that the prepared nanogel exhibited an extensive wound healing response when compared to the control and marketed gels, as reported by S. Murthy et al., [55].

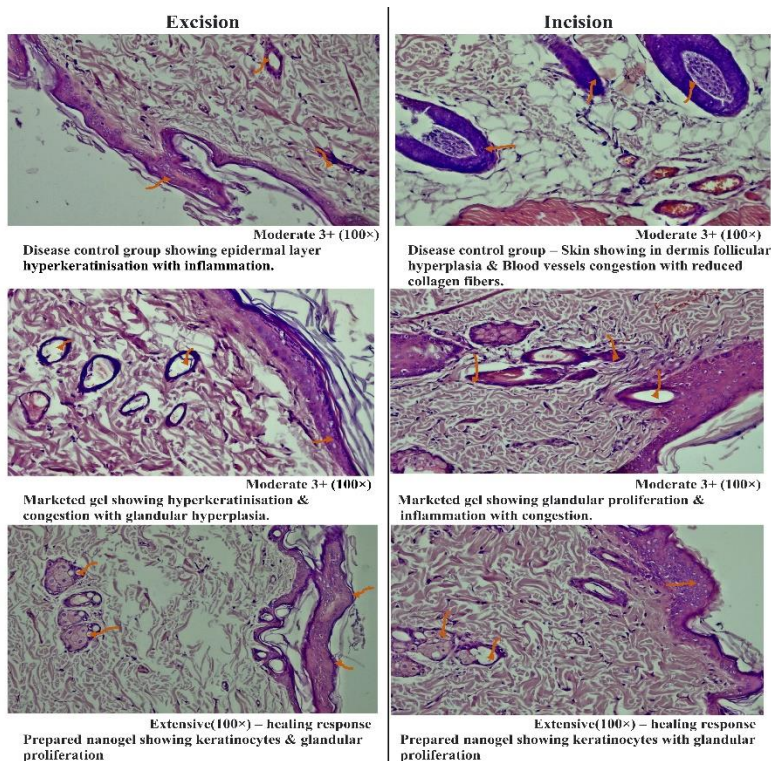


Figure 6 .Represents the histopathology photographs of excision and Incision wound healing activity of nanogel in comparison with marketed and disease control on wistar rats

Biochemical Assays

Hydroxyproline is a key component of collagen and serves as a biomarker for collagenases in the skin tissue. The graph shown in (Figure 7) illustrates the levels of hydroxyproline in the wound tissue of rats administered the marketed gel, prepared nanogel (F3), and no treatment. The results demonstrate that the hydroxyproline content in the wound tissue of the groups treated with each of the two formulations was significantly higher than that of the no treatment groups in both the excision and incision wound models. Notably, the group treated with nanogel (F3) showed a significantly higher amount of hydroxyproline than the untreated and marketed gel groups. Among the three groups, the highest level of hydroxyproline was observed in the group treated with prepared nanogel (F3) (Excision- 243 ± 1.0 and Incision- 128.3 ± 0.6). Furthermore, compared to the other two groups, the hydroxyproline content in the group treated with the marketed formulation was significantly lower (Excision- 213.4 ± 1.0 and Incision- 105 ± 0.7) than in the group treated with the prepared nanogel. The lowest hydroxyproline content was observed in the untreated group (Excision- 125 ± 0.3 and Incision- 74.7 ± 0.5) than in the other groups. Based on the study of hydroxyproline levels in both the excision and incision wound models, it can be concluded that the prepared nanogel (F3) is an effective choice for wound healing as reported by Verma et al., [51].

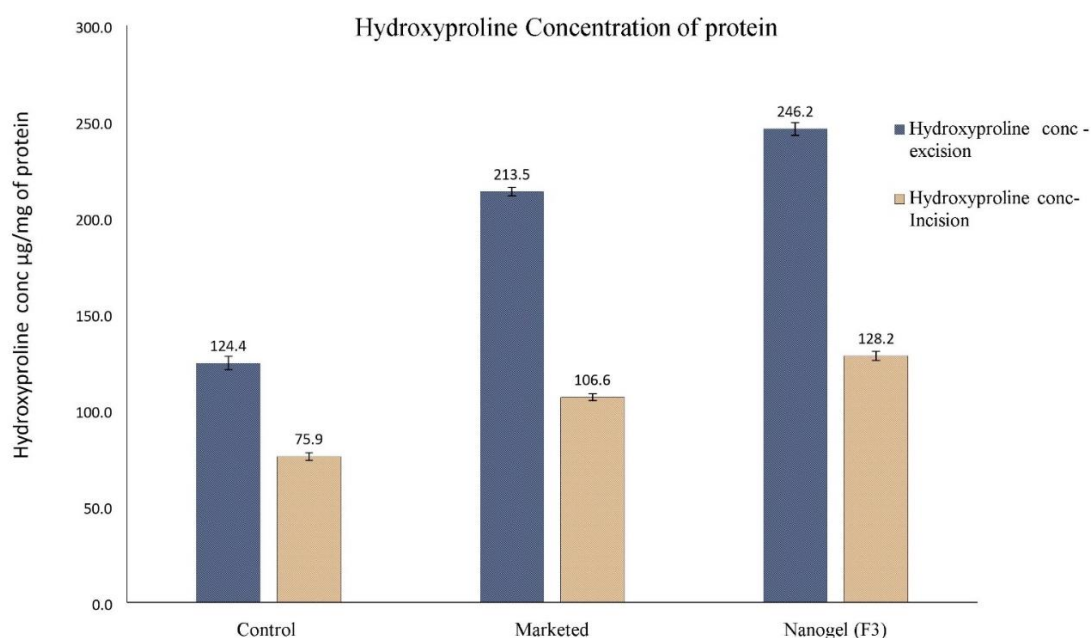


Figure 7. Graphical representation of Hydroxyproline concentration

Stability studies

A stability study was carried out to assess the behavior of the nanogel, and the results indicated that there were no substantial variations in its physical or content uniformity throughout storage (Table 3). Therefore, it can be concluded that the nanogel exhibited excellent stability within the specified time frame.

Table 3. Stability study data for Nanogel formulations

Days	Appearance	PH	Viscosity	
			RPM	CPS
0 day	Brown-colored homogenous	6.1 ± 0.02	RPM 5	8879 ± 7.0
			RPM 10	4386 ± 3.6
			RPM 20	2825 ± 3.1
			RPM 50	2161 ± 4.0
			RPM 100	1693 ± 6.2
30 days	Brown-colored homogenous	6.2 ± 0.03	RPM 5	8858 ± 7.2
			RPM 10	4373 ± 6.8
			RPM 20	2919 ± 1.0
			RPM 50	2155 ± 9.0
			RPM 100	1682 ± 4.2
60 days	Brown-colored homogenous	6.2 ± 0.01	RPM 5	8854 ± 4.7
			RPM 10	4390 ± 6.0
			RPM 20	2932 ± 8.7
			RPM 50	2151 ± 7.2
			RPM 100	1678 ± 8.7
120 days	Brown-colored homogenous	6.1 ± 0.02	RPM 5	8864 ± 3.5
			RPM 10	4391 ± 9.2
			RPM 20	2927 ± 6.7
			RPM 50	2158 ± 7.8
			RPM 100	1690 ± 2.1
180 days	Brown-colored homogenous	6.1 ± 0.04	RPM 5	8860 ± 6.8
			RPM 10	4382 ± 5.9
			RPM 20	2930 ± 6.4
			RPM 50	2159 ± 9.0
			RPM 100	1681 ± 9.5

4. Conclusion

The primary aim of this research was to explore the optimization and production of a morinda citrifolia and sericin nanogel combination for the purpose of accelerating wound healing.Initially, Morinda citrifolia leaf extract and sericin from silk cocoons were extracted. The nanogel was optimized using the solvent diffusion method with carbopol-940 and HPMC as gelling agents, and its various characteristics, such as pH, spreadability, swelling index, water absorption, extract content, particle size, PDI, and an Invitro release study were studied. The cytotoxicity study showed no signs of toxicity in the formulation using HDF, and the wound scratch assay demonstrated better values compared to the standard. F3 formulation exhibited very good results when tested Invivo. Skin irritation studies showed no signs of toxicity after topical application, and hence it is concluded the nanogel was safe for use. Excision and incision studies revealed favorable results for the nanogel compared with the marketed gel, and it also showed a better hydroxyproline profile than the marketed gel. Therefore, based on these studies, the preliminary nanogel (F3) appears to have a superior wound healing effect.

Funding Details

The author express their heartfelt gratitude to the management of M S Ramaiah University of Applied Sciences, Bengaluru, India for awarding the junior Research Fellowship (RUAS/RD/2023/020). This generous support has facilitated the seamless execution of the *Nanotechnology Perceptions* Vol. 20 No. S8 (2024)

research.

Acknowledgements

We acknowledge Central Silk Board Institute, Bengaluru, Karnataka and New Life herbal products for providing fresh bombyx mori silk cocoons, morinda citrifolia leaf. We gratefully acknowledge Indian Institute of Science, Bengaluru and Sitra Laboratory Chennai for providing various analytical facilities for characterization studies. Authors are thankful to Averin Biotech Labs, Bengaluru and Biocorpsscintific, Hyderabad for performing In vitro cell line studies. The authors are grateful to Faculty of pharmacy, M S Ramaiah University of Applied Sciences, Bengaluru for providing necessary support for the study.

Declarations

Conflict of Interest

No conflict of interest

Data Availability All the data generated or analysed during the study are included in this publication article [and its supplementary information files].

References

1. Thakur, R., Jain, N., Pathak, R., & Sandhu, S. S. (2011). Practices in wound healing studies of plants. *Evidence-Based Complementary and Alternative Medicine*, 2011. <https://doi.org/10.1155/2011/438056>
2. Takeo, M., Lee, W., & Ito, M. (2015). Wound healing and skin regeneration. *Cold Spring Harbor Perspectives in Medicine*, 5(1), 1–12. <https://doi.org/10.1101/cshperspect.a023267>
3. Tottoli, E. M., Dorati, R., Genta, I., Chiesa, E., Pisani, S., & Conti, B. (2020). Skin wound healing process and new emerging technologies for skin wound care and regeneration. *Pharmaceutics*, 12(8), 1–30. <https://doi.org/10.3390/pharmaceutics12080735>
4. Mihaela georgescu, Oana m, Marcela P, Teodora stan, veronica. (2016). Natural compounds for wound healing. *Intech open science*, 2016. <https://www.intechopen.com/books/advanced-biometric-technologies/liveness-detection-in-biometrics>
5. Vandervord, J. G., Tolerton, S. K., Campbell, P. A., Darke, J. M., & Loch-Wilkinson, A. M. V. (2016). Acute management of skin tears: A change in practice pilot study. *International Wound Journal*, 13(1), 59–64. <https://doi.org/10.1111/iwj.12227>
6. Idris Adewale Ahmed. *Ethnomedicinal Uses of Some Common Malaysian Medicinal Plants, Natural Drugs from Plants*, 2012. <https://doi.org/10.1016/j.colsurfa.2011.12.014>
7. Wilkinson, H. N., & Hardman, M. J. (2023). Wound healing: Cellular mechanisms and pathological outcomes. *Advances in Surgical and Medical Specialties*, 341–370. <https://doi.org/10.1098/rsob.200223>
8. Hosseinkhani, A., Falahatzadeh, M., Raoofi, E., & Zarshenas, M. M. (2017). An Evidence-Based Review on Wound Healing Herbal Remedies From Reports of Traditional Persian Medicine. *Journal of Evidence-Based Complementary and Alternative Medicine*, 22(2), 334–343. <https://doi.org/10.1177/2156587216654773>
9. Pushparani, D. S., Hemalatha, R., Nivethitha, D. K., & Pushpanjali, C. (2018). Role of Herbal Extracts in Wound Healing Process A Review. *International Journal of ChemTech Research*, 11(10), 280–286. <https://doi.org/10.20902/ijctr.2018.111034>
10. Isolation, Purification and Characterization of Sericin Protein from the Discharge Water of Silk Industry. *Madras Agric J*. 2020; 107:1–6.

11. Miyada, D. S., & Tappel, A. L. (1956). Colorimetric determination of hydroxyproline. *Analytical Chemistry*, 28(5), 909–910. <https://doi.org/10.1021/ac60113a039>
12. Ignat'eva, N. Y., Danilov, N. A., Averkiev, S. V., Obrezkova, M. V., Lunin, V. V., & Sobol', E. N. (2007). Determination of hydroxyproline in tissues and the evaluation of the collagen content of the tissues. *Journal of Analytical Chemistry*, 62(1), 51–57. <https://doi.org/10.1134/S106193480701011X>
13. Wilkinson HN, Hardman M.J. Wound healing.(2023). Cellular mechanisms and pathological outcomes. *Adv Surg Med Spec*. 2023; 341–70. <https://doi.org/10.1098/rsob.200223> .
14. Rivera, A., Cedillo, L., Hernández, F., Castillo, V., Sánchez, A., & Castañeda, D. (2012). Bioactive constituents in ethanolic extract leaves and fruit juice of *Morinda citrifolia*. 3(2), 1044–1049.
15. Nayak, B. K., Suchitra, V., & Nanda, A. (2015). Antibacterial potency of hydro-alcohol leaf extract of *Morinda citrifolia* L. (Noni) by soxhlet extraction method. *Der Pharmacia Lettre*, 7(4), 51–54.
16. Sang, S., Cheng, X., Zhu, N., Stark, R. E., Badmaev, V., Ghai, G., Rosen, R. T., & Ho, C. T. (2001). Flavonol glycosides and novel iridoid glycoside from the leaves of *Morinda citrifolia*. *Journal of Agricultural and Food Chemistry*, 49(9), 4478–4481. <https://doi.org/10.1021/jf010492e>
17. S Tole S.B, Demgunde N.D, Joshi A.A, Korekar S.L “Formulation of Morinda Wound Healing Ointment.” *International Journal of Management and Humanities*, 4(9), 80–84. <https://doi.org/10.35940/ijmh.i0895.054920>
18. Arul Kumaran. (2017).Development and characterization of morinda citrifolia phytosomal gel for topical master of pharmacy (Pharmaceutics) (Pharmaceutics) APRIL-2017.
19. Kunz, R. I., Brancalhão, R. M. C., Ribeiro, L. D. F. C., & Natali, M. R. M. (2016). Silkworm Sericin: Properties and Biomedical Applications. *BioMed Research International*, 2016. <https://doi.org/10.1155/2016/8175701>
20. Gupta, D., Agrawal, A., & Rangi, A. (2014). Extraction and characterization of silk sericin. *Indian Journal of Fibre and Textile Research*, 39(4), 364–372.
21. Harsulakar, A. A. (2022). Design, Development and Characterization of Nanogel Containing Herbal Drug. 9(6), 81–95.
22. Srinivas, P. R., Philbert, M., Vu, T. Q., Huang, Q., Kokini, J. L., Saos, E., Chen, H., Peterson, C. M., Friedl, K. E., McDade-Ngutter, C., Hubbard, V., Starke-Reed, P., Miller, N., Betz, J. M., Dwyer, J., Milner, J., & Ross, S. A. (2010). Nanotechnology research: Applications in nutritional sciences. *Journal of Nutrition*, 140(1), 119–124. <https://doi.org/10.3945/jn.109.115048>
23. Suryam Gugulothu. (2023). Formulation and Development of Nanogel Containing Green Tea Extract: As Topical Dosage Form. *World journal of pharmaceutical and medical research*, 2023.273–85. <https://www.wjpmr.com/abstract/5071>.
24. Patra, J. K., Das, G., Fraceto, L. F., Campos, E. V. R., Rodriguez-Torres, M. D. P., Acosta-Torres, L. S., Diaz-Torres, L. A., Grillo, R., Swamy, M. K., Sharma, S., Habtemariam, S., & Shin, H. S. (2018). Nano based drug delivery systems: Recent developments and future prospects. *Journal of Nanobiotechnology*, 16(1), 1–33. <https://doi.org/10.1186/s12951-018-0392-8>
25. Singh, S., Sonia, Sindhu, R. K., Alsayegh, A. A., Batiha, G. E. S., Alotaibi, S. S., Albogami, S. M., & Conte-Junior, C. A. (2023). Formulation Development and Investigations on Therapeutic Potential of Nanogel from *Beta vulgaris* L. Extract in Testosterone-Induced Alopecia. *BioMed Research International*, 2023. <https://doi.org/10.1155/2023/1777631>
26. Anooj, E. S., Charumathy, M., Sharma, V., Vibala, B. V., Gopukumar, S. T., Jainab, S. I. B., & Vallinayagam, S. (2021). Nanogels: An overview of properties, biomedical applications, future research trends and developments. *Journal of Molecular Structure*, 1239, 130446. <https://doi.org/10.1016/j.molstruc.2021.130446>

27. Aparna C. (2022). A Review on Nanogels Aparna C*, Prasanna N. 1–9. <https://doi.org/10.36648/1791-809X-14.09-973>
28. Binh, D., Pham Thi Thu Hong, Nguyen Ngoc Duy, Nguyen Thanh Duoc, & Nguyen Nguyet Dieu. (2012). A study on size effect of carboxymethyl starch nanogel crosslinked by electron beam radiation. *Radiation Physics and Chemistry*, 81(7), 906–912. <https://doi.org/10.1016/j.radphyschem.2011.12.016>
29. Geetha, D., Jayashree, I., & Rajeswari, M. (2019). Gc-Ms Analysis of Bioactive Compounds of Ethanolic Seed Extract of *Elaeocarpus Serratus*. *International Journal of Pharmaceutical Sciences and Drug Research*, 11(1), 31–34. <https://doi.org/10.25004/ijpsdr.2019.110105>
30. Ahmed, A. B., Tahir, H. M., Yousaf, M. S., Munir, F., & Ali, S. (2023). Efficacy of Silk Sericin and *Jasminum grandiflorum* L. Leaf Extract on Skin Injuries Induced by Burn in Mice. *Journal of Burn Care & Research : Official Publication of the American Burn Association*, 44(1), 58–64. <https://doi.org/10.1093/jbcr/irac069>
31. Cherng, J. H., Chang, S. J., Chiu, Y. K., Chiu, Y. H., Fang, T. J., & Chen, H. C. (2022). Low Molecular Weight Sericin Enhances the In Vitro of Immunological Modulation and Cell Migration. *Frontiers in Bioengineering and Biotechnology*, 10(July), 1–15. <https://doi.org/10.3389/fbioe.2022.925197>
32. Pawar, A. Y., Jadhav, K. R., Malpure, P. S., Shinkar, D. M., Pingale, M. S., & Sanap, A. S. (2022). Design of Novel Nanogel Formulation of Naproxen Sodium for Enhanced Anti-inflammatory Effect. *Asian Journal of Pharmaceutics*, 16(2), 203.
33. Muniraj S N, Yogananda R, Nagaraja T.S.(2020). Preparation and Characterization of Nanogel Drug Delivery System Containing Clotrimazole an Anti-Fungal Drug". *Indo American Journal of Pharmaceutical Research*, 10(07), 2020. www.iajpr.com
34. Sabirin, I. P. R., & Yuslianti, E. R. (2016). Benefits of Ethanolic Extract Paste of Noni (*Morinda citrifolia* L.) Leaves on Oral Mucosa Wound Healing by Examination of Fibroblast Cells. *Journal of Dentistry Indonesia*, 23(3), 59–63. <https://doi.org/10.14693/jdi.v23i3.980>
35. Munir, F., Tahir, H. M., Ali, S., Ali, A., Tehreem, A., Zaidi, S. D. E. S., Adnan, M., & Ijaz, F. (2023). Characterization and Evaluation of Silk Sericin-Based Hydrogel: A Promising Biomaterial for Efficient Healing of Acute Wounds. *ACS Omega*, 8(35), 32090–32098. <https://doi.org/10.1021/acsomega.3c04178>
36. Maslii, Y., Ruban, O., Kasparaviciene, G., Kalveniene, Z., Materiienko, A., Ivanauskas, L., Mazurkeviciute, A., Kopustinskiene, D. M., & Bernatoniene, J. (2020). The Influence of pH Values on the Rheological, Textural and Release Properties of Carbomer Polacril 40P-Based Dental Gel Formulation with Plant-Derived and Synthetic Active Components. *Molecules (Basel, Switzerland)*, 25(21). <https://doi.org/10.3390/molecules25215018>
37. Inamdar, Y. M., Rane, B., & Jain, A. (2018). Preparation and Evaluation of Beta sitosterol Nanogel: A Carrier Design for Targeted Drug Delivery system. *Asian Journal of Pharmaceutical Research and Development*, 6(3), 81–87. <https://doi.org/10.22270/ajprd.v6i3.390>
38. Kimbonguila, A., Matos, L., Petit, J., Scher, J., & Nzikou, J.-M. (2019). Effect of Physical Treatment on the Physicochemical, Rheological and Functional Properties of Yam Meal of the Cultivar “Ngumvu” From *Dioscorea Alata* L. of Congo. *International Journal of Recent Scientific Research*, 10(August), 30693–30695. <https://doi.org/10.24327/IJRSR>
39. Afreen, U., Fafelelbom, K. M., Shah, S. N. H., Ashames, A., Almas, U., Khan, S. A., Yameen, M. A., Nisar, N., Asad, M. H. H. Bin, & Murtaza, G. (2022). Formulation and evaluation of niosomes-based chlorpheniramine gel for the treatment of mild to moderate skin allergy. *Journal of Experimental Nanoscience*, 17(1), 467–495. <https://doi.org/10.1080/17458080.2022.2094915>
40. Shoukat, H., Pervaiz, F., Khan, M., Rehman, S., Akram, F., Abid, U., Noreen, S., Nadeem, M., Qaiser, R., Ahmad, R., & Farooq, I. (2022). Development of β -cyclodextrin/polyvinylpyrrolidone-co-poly (2-acrylamide-2-methylpropane sulphonic acid) hybrid nanogels as nano-drug delivery carriers to enhance the solubility of Rosuvastatin: An in

- vitro and in vivo evaluation. PLoS ONE, 17(1 January), 1–28. <https://doi.org/10.1371/journal.pone.0263026>
41. Suhail, M., Fang, C. W., Chiu, I. H., Khan, A., Wu, Y. C., Lin, I. L., Tsai, M. J., & Wu, P. C. (2023). Synthesis and Evaluation of Alginate-Based Nanogels as Sustained Drug Carriers for Caffeine. ACS Omega, 8(26), 23991–24002. <https://doi.org/10.1021/acsomega.3c02699>
42. Pallab, K., Tapan K, B., Tapas K, P., & Ramen, K. (2011). Research Article Estimation of Total Flavonoids Content (Tfc) and Anti Oxidant Activities of Methanolic Whole Plant Extract of Biophytum Sensitivum Linn. Journal of Drug Delivery and Therapeutics, 10(1), 33–37.
43. Rao Avanapu, S., & Rao, As. (2014). Design and invitro Evaluation of Nanogel Containing Mentha piperita. American Journal of Biological and Pharmaceutical Research, 1(3), 136–139. <https://www.researchgate.net/publication/284173316>
44. Christodoulou, I., Goulielmaki, M., Kritikos, A., Zoumpourlis, P., Koliakos, G., & Zoumpourlis, V. (2022). Suitability of Human Mesenchymal Stem Cells Derived from Fetal Umbilical Cord (Wharton’s Jelly) as an Alternative In Vitro Model for Acute Drug Toxicity Screening. Cells, 11(7). <https://doi.org/10.3390/cells11071102>
45. Syarina, P. N. A., Karthivashan, G., Abas, F., Arulselvan, P., & Fakurazi, S. (2015). Wound healing potential of spirulina platensis extracts on human dermal fibroblast cells. EXCLI Journal, 14(May), 385–393. <https://doi.org/10.17179/excli2014-697>
46. Arollado, E. C., Samaniego, A. A., Cena, R. B., Agapito, J. D., Tomagan, L. B., Ponsaran, K. M. G., Manalo, R. A. M., & Dela Torre, G. L. T. (2018). Cocos nucifera L. Endosperm promotes healing of excised wound in BALB/C mice. Marmara Pharmaceutical Journal, 22(1), 103–109. <https://doi.org/10.12991/mpj.2018.48>
47. Patel, N., Patel, N. A., Patel, M., & Patel, R. P. (2011). Formulation and Evaluation of Polyherbal Gel for Wound Healing. Intl. R. J. of Pharmaceuticals, 01(August), 15–20. www.scientific-journals.co.uk
48. Wang, Y., Chinnathambi, A., Nasif, O., & Alharbi, S. A. (2021). Green synthesis and chemical characterization of a novel anti-human pancreatic cancer supplement by silver nanoparticles containing Zingiber officinale leaf aqueous extract. Arabian Journal of Chemistry, 14(4), 103081. <https://doi.org/10.1016/j.arabjc.2021.103081>
49. Zangeneh, M. M., Joshani, Z., Zangeneh, A., & Miri, E. (2019). Green synthesis of silver nanoparticles using aqueous extract of Stachys lavandulifolia flower, and their cytotoxicity, antioxidant, antibacterial and cutaneous wound-healing properties. Applied Organometallic Chemistry, 33(9), 1–15. <https://doi.org/10.1002/aoc.5016>
50. Masson-Meyers, D. S., Andrade, T. A. M., Caetano, G. F., Guimaraes, F. R., Leite, M. N., Leite, S. N., & Frade, M. A. C. (2020). Experimental models and methods for cutaneous wound healing assessment. International Journal of Experimental Pathology, 101(1–2), 21–37. <https://doi.org/10.1111/iep.12346>
51. Verma, E., Patil, S., & Gajbhiye, A. (2023). Sequential analysis for identification of byproduct from N-benzoylation reaction: wound healing and anti-inflammatory potential of the byproduct 4-chlorobenzyl 2-((4-chlorobenzyl) amino) benzoate. RSC Advances, 13(37), 25904–25911. <https://doi.org/10.1039/d3ra03720g>
52. Al-Hamadani, M. H., & Al-Edresi, S. (2022). Formulation and Characterization of Hydrogel of Proniosomes Loaded Diclofenac Sodium. International Journal of Drug Delivery Technology, 12(1), 132–136. <https://doi.org/10.25258/ijddt.12.1.24>
53. Ali, A., Ali, A., Rahman, M. A., Warsi, M. H., Yusuf, M., & Alam, P. (2022). Development of Nanogel Loaded with Lidocaine for Wound-Healing: Illustration of Improved Drug Deposition and Skin Safety Analysis. Gels, 8(8). <https://doi.org/10.3390/gels8080466>
54. Seo, S. J., Das, G., Shin, H. S., & Patra, J. K. (2023). Silk Sericin Protein Materials: Characteristics and Applications in Food-Sector Industries. International Journal of Molecular Sciences, 24(5). <https://doi.org/10.3390/ijms24054951>

55. Murthy, S., Gautam, M. K., Goel, S., Purohit, V., Sharma, H., & Goel, R. K. (2013). Evaluation of in vivo wound healing activity of *Bacopa monniera* on different wound model in rats. *BioMed Research International*, 2013. <https://doi.org/10.1155/2013/972028>
56. Abdul Rahman, M. N., Qader, O. A. J. A., Sukmasari, S., Ismail, A. F., & Doolaanea, A. A. (2017). Rheological characterization of different gelling polymers for dental gel formulation. *Journal of Pharmaceutical Sciences and Research*, 9(12), 2633–2640.

Graphical Abstract

